

Paper No.
17007



Adhesion of Corrosion Product Layers Formed in Dewing Conditions

Claudia Prieto, Bruce Brown, Marc Singer, David Young

Institute for Corrosion and Multiphase Technology
Department of Chemical and Biomolecular Engineering
Ohio University, Athens, OH 45701

ABSTRACT

Engineers in the oil and gas industry frequently rely on the formation of protective corrosion product layers to mitigate internal pipeline corrosion. However, their protectiveness can be compromised if such layers, iron carbonate formed during CO₂ corrosion for example, are mechanically removed from the metal. Partial loss of a corrosion product layer has the potential to result in localized attack and loss of containment. In sour environments, this partial loss can lead to particulate (black powder in case of commercial gas pipelines) entrainment, which can cause multiple problems downstream in the pipeline. Consequently, the study of adhesion forces between iron carbonate, iron oxide or iron sulfide layers and their associated metal substrate is essential to the industry. In the current work, adherence characteristics of iron carbonate layers grown in dewing conditions (condensing water conditions) were mechanically characterized *via* scratch testing by measuring the critical force to produce a removal of the layer. With the use of critical frictional forces (tangential forces parallel to the surface that produce the removal of the corrosion product) and the projected area of the indenter, the shear stress associated with the removal of the layer was calculated. This mechanical assessment was extended to layers grown in bulk aqueous conditions for comparative purposes. The results indicated that the critical shear stress for the removal of iron carbonate in dewing conditions was 3 orders of magnitude lower than for iron carbonate grown in aqueous environments. Finally, the critical shear stress for iron sulfide produced in dewing conditions indicated that the layer was significantly more adherent than the iron carbonate layer grown in similar conditions. In addition to understanding corrosion phenomena, this work has significance relating to black powder formation and resultant erosion.

INTRODUCTION

The oil and gas industry produces a large variety of products essential to everyday life, such as gasoline, diesel, and natural gas as fuels as well as petrochemical feedstocks used to make a

wide range of products. To transport refined products as liquids or gases to customers, the oil and gas industry frequently uses transmission pipelines. One of the operational problems associated with gas transmission pipelines is the formation of black powder¹. As its name suggests, black powder is blackish dust that can impact the performance of transportation pipelines due to its accumulation, even resulting in pipelines potentially becoming blocked^{1,2}. This blockage affects the flow of gas, thereby reducing the amount that is delivered to the end user. In terms of pipeline integrity, black powder causes erosion of the internal pipe wall, compromises the functioning of critical components (e.g., sensors, valves), and induces pressure drop due to the variation of internal diameter³. Gas turbine blades are also susceptible to damage caused by black powder accumulation due to excessive wear and erosion³. Therefore, understanding mechanisms of spallation are essential so that conditions at which corrosion products form black powder can be avoided, predicted, or mitigated.

Consequently, if the proposed research determines the tendency of corrosion products on steel to undergo spallation related to evolving stresses with loss of adherence, then this knowledge can potentially be applied for the development of black powder prevention strategies. Also, the proposed research has the potential to add to the understanding of localized corrosion mechanisms associated with local detachment of iron carbonate and iron sulfide layer. Before proceeding to the experimental procedure, the critical points of the theory behind the tribology techniques to assess the mechanical integrity of thin films are discussed.

Cohesive Failures of Thin Layers

Cohesive failure of thin layers can be defined as the partial delamination that can occur within the same layer^{4,5}. This failure usually happens at the gas-layer interface^{4,5}. The most commonly reported forms of cohesive failures are buckling and spallation⁶. Buckling is the cracking and lifting of part of the layer⁶; spallation is the partial removal of small parts of the layer⁶. Partial delamination is generally caused by external agents such as shear stress exerted by a fluid, the internal stresses within the layer, or thermal expansion stresses⁷. Internal stresses refer to the stresses generated within a crystalline layer at deposition or growing due to mismatching of crystals, impingement during their growth, and bonds between crystals⁷.

Adhesive Failures of Thin Layers

This type of failure refers to the total detachment of a thin layer from the substrate⁸. Such a condition is reported to be produced by external mechanical forces such as shear stresses generated with industrial cutting tools^{4,5}. The forces required to produce this type of failure are generally higher than the forces to produce a cohesive failure⁶. The bonding between the film and the substrate plays a governing role in this type of failure, as well as other internal stresses within the layer⁹. Bull, *et al.*, have discussed the contribution of the abovementioned internal stresses in their practical assessment of adhesion of thin layers¹⁰. Regarding studies of corrosion product layers, in past research conducted on the forces required to remove iron carbonate product layers, Yang, *et al.*, used tensile strength testing to determine the layer removal forces from a mild steel surface. They reported values in the order of MPa to remove an iron carbonate layer¹¹. Xiong, *et al.*, reported similar values for the removal of a single crystal of iron carbonate with atomic force microscopy (AFM)¹².

Scratch Adhesion Testing Theory

Scratch testing is a tribological technique widely utilized, among other applications, in the determination of adhesive forces between a substrate and thin layers^{10,13,14}. This technique is considered a robust method to obtain information about the adhesion of a film to a substrate^{10,15}. The method can capture the three primary contributing parameters that govern the adhesion phenomena between a thin film/coating/layer and a substrate: internal stresses within the film, the adhesive friction between the stylus and the contacted surface, and the plowing contribution of the indenter.

Burnett, Rickerby, and Bull utilized the fundamental approach followed by Laugier¹⁶ (energy balance approach) to identify three main forces contributing to the layer detachment: elastic-plastic indentation stress, internal stresses, and tangential frictional stress as shown in Figure 1¹⁰.

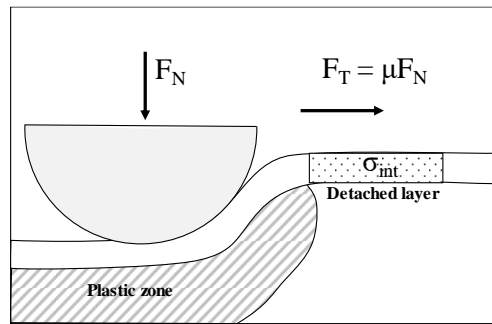


Figure 1. Three main contributors for the detachment of layers on a substrate: plowing component (a function of F_N), internal stress component (σ_{int}), and tangential force (F_T). μ is the friction coefficient of the layer. Adapted from Burnett, *et al.*¹⁷

Bull, *et al.*, also proposed that the friction forces measured by the scratch adhesion test can be represented as the sum of the three contributors (elastic-plastic indentation, internal stresses and frictional stress) under the premise that the indentation term produces a tangential force as a function of the friction coefficient, and the internal stresses add an extra resistance tangential force¹⁰. Moreover, Bull, *et al.*, also distinguished the adhesive failures produced by tensile forces and failures produced by compressive forces⁶. This type of failure depends on the nature of interaction of the layer and the substrate and can be detected by microscopy^{6,14}. Therefore, a microscopic inspection must be performed before choosing the model equation to obtain the critical shear stress for failures. If the failure is governed by compressive stresses, the shear stress is given by:

$$\tau_c = \frac{F_T}{A} \quad (1)$$

Where τ_c is the critical shear stress to produce failure, F_T is the tangential force of plowing, as defined in Figure 1, and A is the area where the tangential force was acting on the layer.

Whereas if the tensile stress is causing the detachment of the layer, the model equation for the critical shear stress (τ_t) is given by:

$$\tau_t = \frac{\nu_l F_T}{A} \quad (2)$$

Where ν_l is the Poisson ratio of the layer.

The Case for Flexible Substrates and Brittle Coatings

Ollivier and Matthews (O&M) simplified the energy criterion proposed by Bull and developed a mathematical model for hard thin films deposited on a flexible substrate¹⁸. Although simple, this model is in good agreement with the experimental observations of Laugier, Perry, and Weaver¹⁹⁻²¹. They argued that the forces during a scratch test can be modeled by a quasi-static approach as depicted by Figure 2. Figure 2 shows the geometrical parameters and forces involved in the determination of the tangential force to transform it into a shear stress value. Under this assumption, the layers experience adhesive failure when a normal load (P : orange vector in Figure 2) in conjunction with its associated tangential force (the red vector in Figure 2, F) is reached. Such a normal load is called the critical load. Moreover, the authors assumed that, at the critical load, the plastic deformation of the substrate is negligible for flexible substrates. A flexible substrate can be defined as a substrate that exhibit elastic strain recovery in the range of working forces with a minimum of plastic deformation¹⁸. There are also two implicit assumptions: internal stresses are negligible, and the scratch testing process is performed quasi-statically. In other words, the process occurs so slowly that the static analysis of the forces is valid. Consequently, the tangential force is a linear function of the normal force, independent from the substrate.

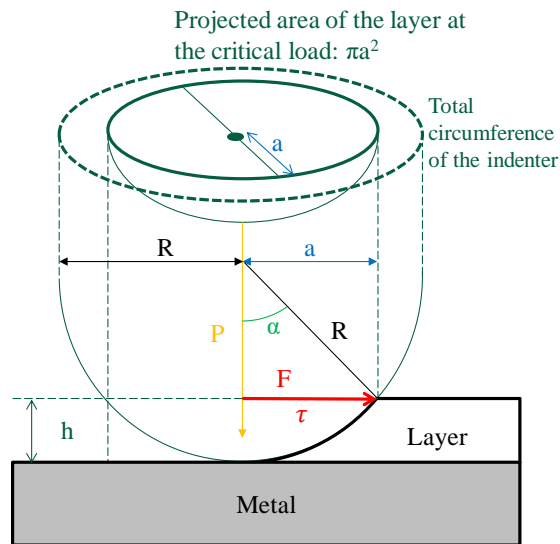


Figure 2. The principle of scratching to remove a layer (white) from a metal substrate (gray). Related physical magnitudes are colored-related. P is the vertical load of the indenter, related to the load (orange-colored). F is the tangential force and τ the shear stress (red). R is the total radius of the indenter; a is the radius at the critical load (when the indenter reached the metal substrate); h is the thickness of the layer.

The mathematical development of the formula is based upon the combination of geometrical parameters and the previously-mentioned forces, as discussed elsewhere¹⁸. The result is a formula that transforms the critical load into tangential forces and shear stress:

$$F_T = F_N \frac{a}{\sqrt{R^2 - a^2}} \quad (3)$$

At the critical load, $F_N = L_c$, thereby:

$$\tau = \frac{L_c}{\pi a \sqrt{R^2 - a^2}} \quad (4)$$

EXPERIMENTAL PROCEDURE

Table 1 shows the experimental conditions at which the iron carbonate layers were formed.

Table 1. Test Matrix for Iron Carbonate Formation

Parameter	Value	
Temperature of solution / °C	80	
Sparge gas	CO ₂	
Working solution	1 wt.% NaCl	
Material	X65	
pH	8.0 ± 0.2	6.6
Fe ²⁺ initial concentration / ppm	50	100
Test duration	3 days	

Formation of Layers in Dewing Conditions

Table 2 shows the parameters to obtain iron carbonate layers in dewing conditions, and Table 3 shows the experimental conditions to form an iron sulfide in dewing conditions.

Table 2. Test Matrix for Iron Carbonate Formation in Dewing Conditions

Parameter	Value
Steel substrate	X65
Temperature of steel / °C	60
Temperature of the gas / °C	75
Sparge gas	0.62 bar CO ₂ (0.38 bar H ₂ O vapor pressure balance)
Working solution	Condensate water (calculated bulk pH ≈ 4.0)
Test duration	3 days

Table 3. Test Matrix for Iron Sulfide in Dewing Conditions

Parameter	Value
Steel substrate	X65
Temperature of steel / °C	30
Temperature of the gas / °C	35
Sparge gas	H ₂ S/N ₂ mixed gas (100 ppm _v H ₂ S)
Working solution	Condensate water (calculated bulk pH ≈ 6.0)
Test duration	3 days

The gas and solution temperature were chosen based upon the work published by Colahan, *et al*²², since iron carbonate and iron sulfide layers were successfully developed at such conditions. X-ray diffraction (XRD) was used to corroborate corrosion product formation. The test apparatus

was a glass cell setup with a Peltier thermoelectric system utilized to control the temperature of the steel through a PID controller; this was also developed by Colahan, *et al*²². A layout of the glass cell is shown in Figure 3.

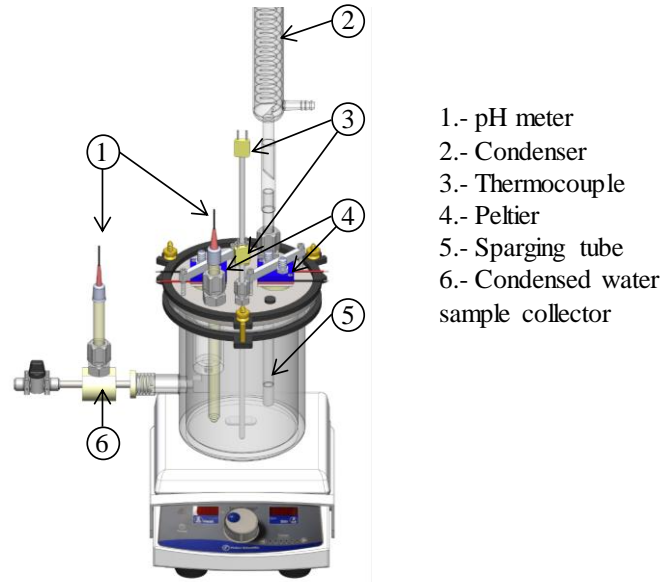


Figure 3. Glass cell apparatus to obtain corrosion product layers under dewing conditions.

Adhesive Properties of Corrosion Product Layers

Scratch testing was utilized to assess the adherence forces of the corrosion product layers. Table 4 shows the conditions at which the tests were performed.

Table 4. Progressive and Constant Load Scratch Test Parameters

Parameter	Values
Type of Load	Progressive, Constant
Progressive Load (mN)	0.1 to 800
Constant Loads (mN)	100, 200, 250, 300, 350, 380, 390
Scratch Length (mm)	0.5, 2, 3
Scratching Speed (mm/min)	2
Indenter Geometry	120° Cone
Indenter Material	Diamond
Indenter Tip Radius (µm)	20
Chemical and Optical Characterization	SEM, EDS, Optical Microscopy, Profilometry

Procedure to Determine the Adhesion Forces and Critical Shear Stress via Scratch Testing

This research utilized the methodology described by Bull, *et al.*,⁶ to determine the critical shear stress for iron carbonate removal; therefore, the following steps were followed for the overall assessment of the adherence of corrosion product layers on the X65 steel:

1. Perform a progressive load scratch test to find the mode of failure of the layer on the substrate.
2. Estimate the critical load force from the progressive load scratch test by using Equation (4) and Figure 4.
3. Compare the values obtained with Equation (1) to validate the Ollivier and Matthews model.

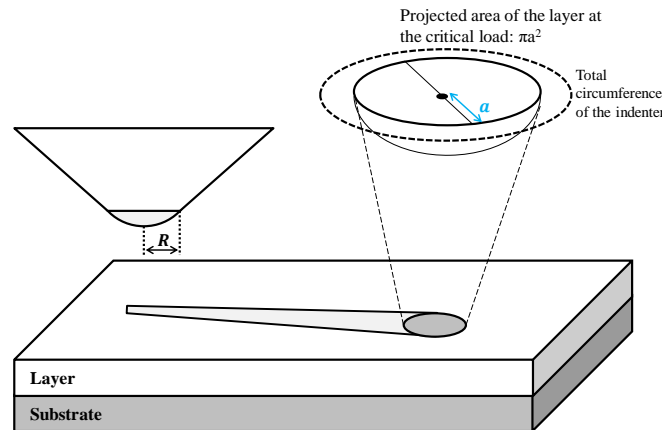


Figure 4. The principle of scratching to remove a layer (white) from a substrate (gray). The indenter cone has a radius “R.” After the scratch, the projected area for the layer removal (πa^2) has a radius “a.” These geometrical parameters are used to calculate the critical shear stress as per Equation (4)¹⁸.

RESULTS AND DISCUSSION

FeCO₃ in Dewing Conditions

Figure 5 shows the iron carbonate layer formed under dewing conditions corroborated by energy dispersive X-ray spectroscopy (EDS) chemical compositional analysis. The layer is discontinuous, and the crystals are smaller in comparison to the fully developed layer in an aqueous environment. The difference can be attributed to the level of saturation of iron carbonate with respect to its precipitation as fully described elsewhere¹¹. Under dewing conditions, the saturation level is higher due to low ionic strength¹¹. A high saturation level might lead to multiple nucleation points on the surface, limiting the growth in size of the crystals.

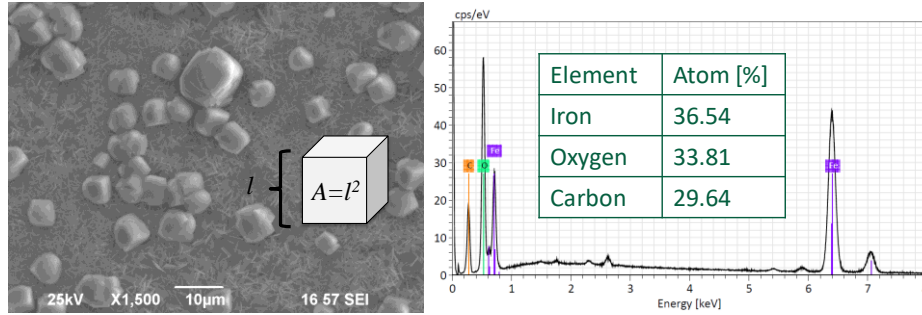


Figure 5. Iron carbonate layers formed under dewing conditions. Average crystal's size: $17 \pm 10 \mu\text{m}^2$. EDS chemical composition analysis is consistent with the presence of iron carbonate.

Scratch testing was performed until a critical load was found (associated with the detachment of the layer) at 2 mN of normal force. A constant load type of scratch test was performed to corroborate the critical failure (detachment of crystals) as illustrated by Figure 6. The critical shear stress was $150 \pm 20 \text{ kPa}$.

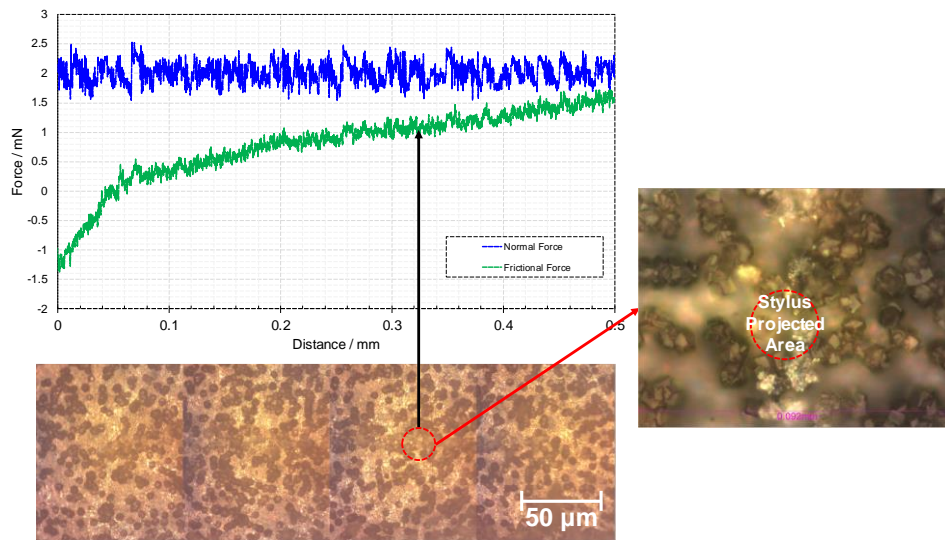


Figure 6. Determination of the critical shear stress of an iron carbonate layer formed under dewing conditions by constant load scratch testing at 2 mN. Critical shear stress: $150 \pm 20 \text{ kPa}$.

FeCO₃ in Aqueous Conditions

Figure 7 shows the morphology of the crystals grown in aqueous conditions at different pH values. Figure 7a shows the crystals formed at pH 6.6. The pH influenced the crystal size of the iron carbonate since at pH 8.0 the level of saturation is higher than at pH 6.6. The average crystal area is of the order of $90 \mu\text{m}^2$, whereas Figure 7b shows that the crystal area for an iron carbonate layer grown at pH 8.0 is, on average, *ca.* $30 \mu\text{m}^2$.

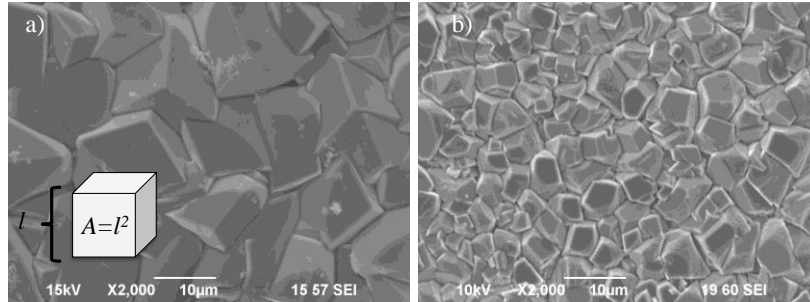


Figure 7. The crystal size of iron carbonate layers at different bulk pH; a) pH 6.6, average crystal's area: $90 \pm 10 \mu\text{m}^2$; pH 8.0, average crystal's area: $29 \pm 9 \mu\text{m}^2$.

Such a change in crystal size is reflected in the critical shear stress to produce a detachment (adhesive failure) from the substrate. As illustrated in Figure 8, the critical force for layer detachment at pH 6.6 ($320 \pm 10 \text{ mN}$) was higher than the critical force for a higher pH ($280 \pm 10 \text{ mN}$). Consequently, the shear stress for detachment of the layer formed at lower pH was larger. This result suggested that the critical shear stress was a function of the crystal's area. One possible explanation is that the size of the crystals grown on the metal substrate plays a governing role in the adherence properties of the layer. A larger contact area between a single crystal and the substrate would lead to a consequent higher adherence force.

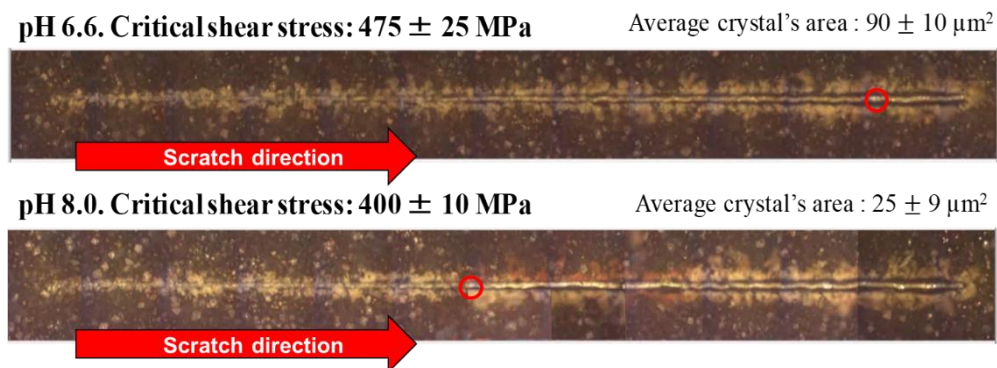


Figure 8. Critical shear stress to produce detachment of the iron carbonate layer grown at different bulk pH. Red circles indicate where the failure was detected.

The comparison of critical shear stress to produce an adhesive failure in an iron carbonate layer grown at different conditions is shown in Figure 9. The critical shear stress to produce an adhesive failure of the layers in dewing conditions was almost three orders of magnitude lower than the critical shear stress for corrosion products developed in aqueous conditions. Moreover, the obtained values are at least three orders of magnitude above the shear stress generated in turbulent flow in pipelines²³. For instance, Li, *et al*²³, experimentally reproduced the flow conditions experienced by pipelines and measured the associated wall shear stress. The values ranged from 10 to 1000 Pa.

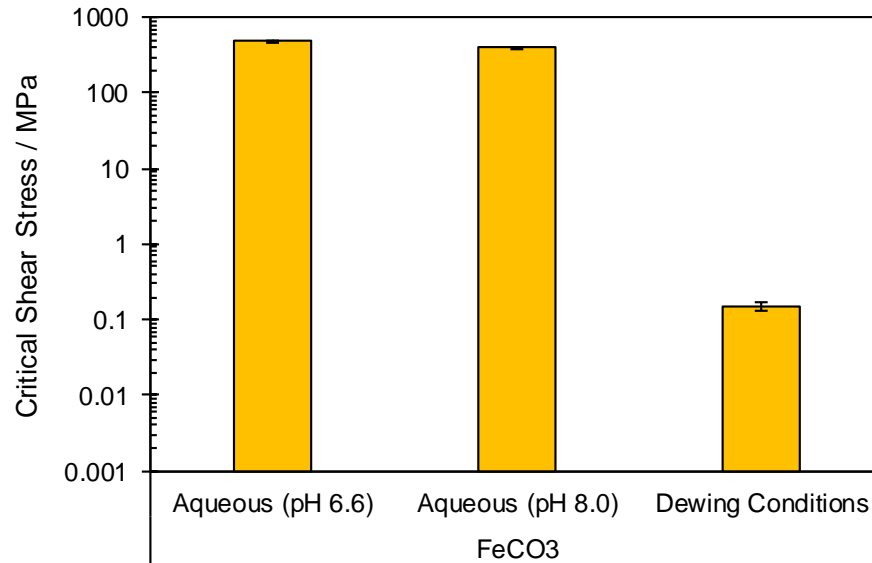


Figure 9. Comparison of critical shear stresses for different iron carbonate layers grown in different conditions.

FeS in Dewing Conditions:

Figure 10 shows the mackinawite layer obtained in dewing conditions. XRD and EDS analysis were performed to confirm its formation.

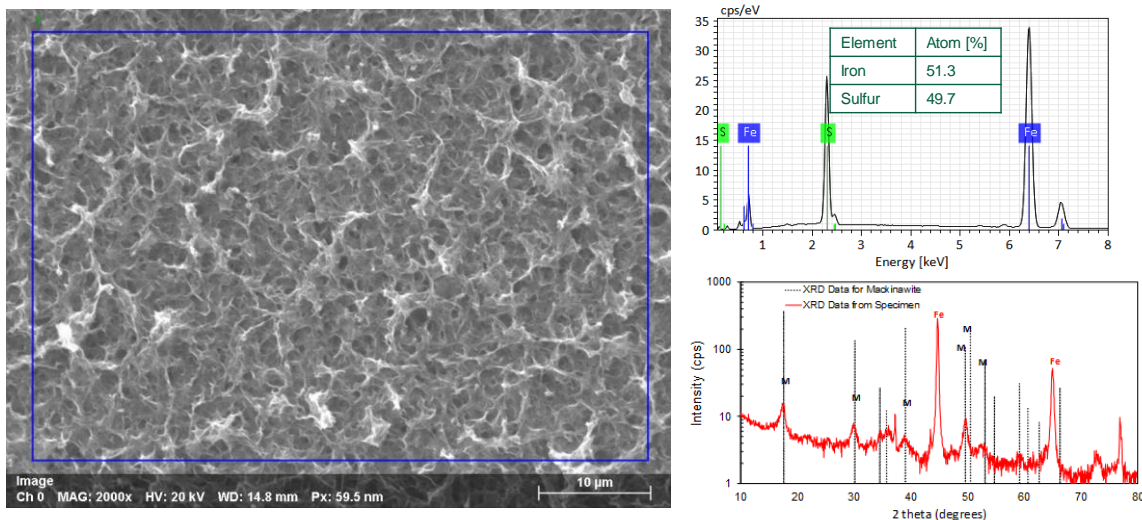


Figure 10. Mackinawite layer confirmed by EDS and XRD analysis.

To characterize the mechanical integrity of the iron sulfide layer, constant load scratch tests were performed at different normal forces which were in the range of 10 to 300 mN. The force that exposes the metal substrate by removing the iron sulfide layer was considered the critical load. In the case of iron sulfide, a 240 mN constant load scratch test produced such an effect. Figure

11 shows that the shear stress associated with the delamination of the layer was of the order of 44 MPa.

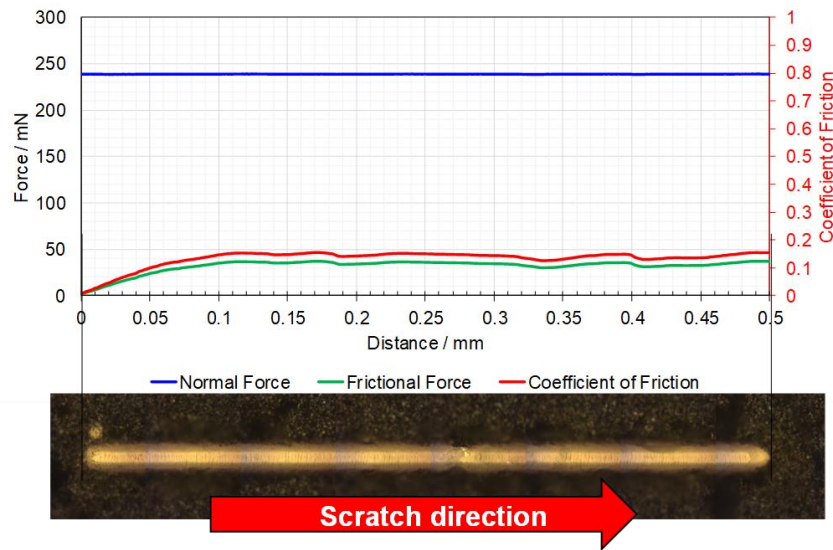


Figure 11. Adhesive failure of the iron sulfide layer in dewing condition. Normal force: 240 mN. Shear stress (by using Equation (1)): 44.2 MPa.

In previous work by Anyanwu, *et al.*,²⁴ the critical shear stress for full delamination of an iron sulfide layer grown under aqueous conditions was determined by using the Ollivier and Matthews approach using a 1018 steel as substrate. The values to delaminate the iron sulfide layers in aqueous conditions from his work were compared to the values to delaminate the iron sulfide layer grown in dewing conditions. Figure 12 shows that the critical shear stress required to produce a failure in a layer grown in an aqueous environment is almost two orders of magnitude higher than that for the layers grown under dewing conditions. Future work will be done to determine if there is an influence in the different substrate for the values.

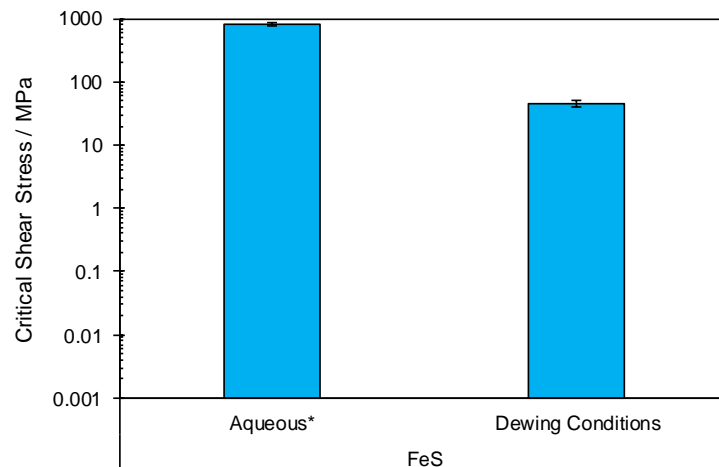


Figure 12. Shear stress for the adhesive failure of a mackinawite layer grown in aqueous conditions²⁴ in a 1018 steel and dewing conditions (x65 steel).

Figure 13 shows the summary of the adhesive properties of iron carbonate and iron sulfide obtained *via* scratch testing.

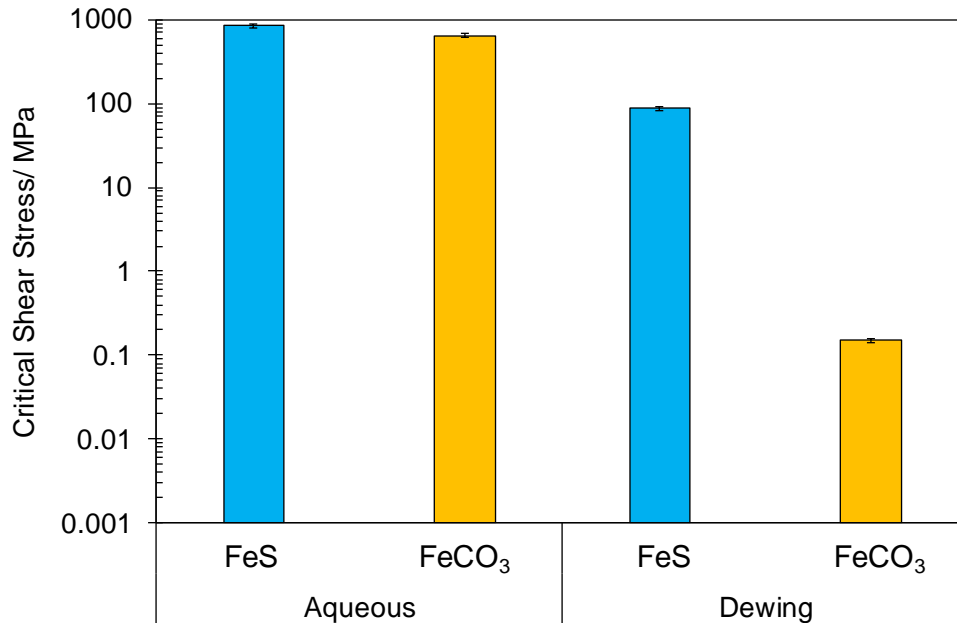


Figure 13. Summary of critical shear stress for different layers grown at aqueous and dewing conditions.

The difference of critical wall shear stress between the iron sulfide and the iron carbonate can be associated with the crystalline nature of the layers. For instance, iron sulfide forms a continuous layer of mackinawite at aqueous and dewing conditions, whereas iron carbonate forms a continuous polycrystalline layer at aqueous conditions, and discrete crystals at dewing conditions. Generally speaking, a continuous layer requires more shear stress to remove than a discrete layer²⁴.

CONCLUSIONS

- Iron carbonate crystals grown in dewing conditions have critical shear stress values three orders of magnitude lower than those grown in aqueous environments.
- Iron carbonate exhibits a lower shear stress resistance with respect to iron sulfide in similar conditions.
- In terms of mechanical integrity of protective layers, it was demonstrated that the layers could not be easily challenged by the shear stress produced by a transported fluid in pipelines, as the values for failure were at least three orders of magnitude higher than the shear stress produced in commercial pipelines. One possible cause for failures might be thermal stresses (expansion and contraction of the substrate due to temperature changes). However, this possibility is outside the scope of this research, but it is suggested for future work.
- Regarding black powder formation, although the shear stress values for cohesive and adhesive failures of layers grown in dewing conditions are significantly lower than layers grown in aqueous conditions, the values were still two to three orders of magnitude higher than the shear stresses typically found in commercial pipelines. Therefore, the formation of black powder is unlikely to be caused by fluid commercial conditions.

ACKNOWLEDGMENTS

The author expresses her gratitude to Dr. Ricardo Nogueira for his valuable comments and discussions.

The authors would like to thank the following companies for their financial support: Petroleum Institute, Anadarko, Baker Hughes, BP, Chevron, Clariant Corporation, ConocoPhillips, DNV GL, ExxonMobil, M-I SWACO (Schlumberger), Multi-Chem (Halliburton), Occidental Oil Company, Pioneer Natural Resources, Saudi Aramco, Shell Global Solutions, SINOPEC (China Petroleum), and TOTAL.

REFERENCES

1. R. M. Baldwin, "Black Powder Problem Will Yield to Understanding, Planning," *Pipeline Gas Ind.*, 1, (1999): pp. 109–112.
2. A. M. Sherik, A. Rasheed, and A. Jabran, "Effect of sales gas pipelines black powder sludge on the corrosion of carbon steel," in NACE Corrosion Conference, 2011, paper 11087 (Houston, TX: NACE, 2011).
3. J. S. Smart, "Black powder movement in gas pipelines," in NACE Corrosion Conference, 2011, paper 11089 (Houston, TX: NACE, 2011).
4. D. Chicot and a Tricoteaux, "Mechanical properties of ceramics by indentation: principle and applications," *Ceram. Mater.*, (2010): pp. 115–153.
5. W. Nix, "Mechanical properties of thin films," *Metall. Mater. Trans. A*, November, (1989): pp. 2217–2245.
6. S. J. Bull, "Failure mode maps in the thin film scratch adhesion test," *Tribol. Int.*, no. 7, (1997): pp. 491–498.
7. P. J. Burnett and D. S. Rickerby, "The mechanical properties of wear-resistant coatings II: experimental studies and interpretation of hardness," *Thin Solid Films*, (1987): pp. 51–65.
8. D. S. Burnett, P. J., Rickerby, "The Relationship Between Hardness and Scratch Adhesion," *Thin Solid Films*, (1987): pp. 403–416.
9. D. Chicot, G. Duarte, A. Tricoteaux, B. Jorgowski, A. Leriche, and J. Lesage, "Vickers Indentation Fracture (VIF) modeling to analyze multi-cracking toughness of titania, alumina and zirconia plasma sprayed coatings," *Mater. Sci. Eng. A*, (2009): pp. 65–76.
10. S. J. Bull, D. S. Rickerby, A. Matthews, A. Leyland, A. R. Pace, and J. Valli, "The use of scratch adhesion testing for the determination of interfacial adhesion: The importance of frictional drag," *Surf. Coatings Technol.*, (1988): pp. 503–517.
11. Y. Yang, B. Brown, and S. Nestic, "Mechanical strength and removal of a protective iron carbonate layer formed on mild steel in CO₂ corrosion," in NACE Corrosion Conference, 2010, paper 10383 (Houston, TX: NACE, 2010).
12. Y. Xiong, B. Brown, B. Kinsella, S. Nestic, and A. Pailleret, "AFM studies of the adhesion properties of surfactant corrosion inhibitor films," NACE Corrosion Conference, 2013, paper 2521 (Houston, TX: NACE, 2013).
13. C. Weaver, "Adhesion of thin films," *J. Vac. Sci. Technol.*, (1975): pp. 18–25.
14. S. J. Bull and E. Berasategui, "An overview of the potential of quantitative coating adhesion measurements by scratch testing," *Tribol. Int.* (2006): pp. 136–165.
15. S. J. Bull and D. S. Rickerby, "New developments in the modelling of the hardness and scratch adhesion of thin films," *Surf. Coatings Technol.*, (1990): pp. 149–164.
16. M. T. Laugier, "An energy approach to the adhesion of coatings using the scratch test," *Thin Solid Films*, (1984): pp. 243–249.
17. P. J. Burnett and D. S. Rickerby, "The scratch adhesion test: an elastic-plastic indentation analysis," *Thin Solid Films*, (1988): pp. 233–254.

18. B. Ollivier and A. Matthews, "Adhesion of diamond-like carbon films on polymers: an assessment of the validity of the scratch test technique applied to flexible substrates," *J. Adhes. Sci. Technol.*, (1994): pp. 651–662.
19. A. J. Perry, "The adhesion of chemically vapour-deposited hard coatings to steel-the scratch test," *Thin Solid Films*, (1981): pp. 77–94.
20. P. Benjamin and C. Weaver, "Measurement of adhesion of thin films," *Proc. R. Soc. London. Ser. A. Math. Phys. Sci.*, (2006): pp. 163–176.
21. M. T. Laugier, "Adhesion of TiC and TiN coatings prepared by chemical vapour deposition on WC-Co-based cemented carbides," *J. Mater. Sci.*, (1986): pp. 2269–2272.
22. M. Colahan, D. Young, M. Singer, and R. P. Nogueira, "Black powder formation by dewing and hygroscopic corrosion processes," *J. Nat. Gas Sci. Eng.*, (2018): pp. 358–367.
23. W. Li, B. F. M. Pots, B. Brown, K. E. Kee, and S. Nesic, "A direct measurement of wall shear stress in multiphase flow - Is it an important parameter in CO₂ corrosion of carbon steel pipelines?" *Corros. Sci.*, (2016): pp. 35–45.
24. E. Anyanwu, C. Prieto, B. Brown, and M. Singer, "mechanical properties of a mackinawite corrosion product layer," in NACE Corrosion Conference, 2019, paper 13441, (Houston, TX: NACE 2019).